

Ni overlayers: many-body excitations

This article has been downloaded from IOPscience. Please scroll down to see the full text article.

1990 J. Phys.: Condens. Matter 2 7853

(<http://iopscience.iop.org/0953-8984/2/38/011>)

View [the table of contents for this issue](#), or go to the [journal homepage](#) for more

Download details:

IP Address: 171.66.16.96

The article was downloaded on 10/05/2010 at 22:31

Please note that [terms and conditions apply](#).

Ni overlayers: many-body excitations

Qibiao Chen, Chanyong Hwang and M Onellion

Physics Department, University of Wisconsin, Madison, WI 53706, USA

Received 20 February 1990, in final form 29 May 1990

Abstract. The electronic band structure of Ni overlayers of 1–5 monolayers (ML) on $\text{Cu}_3\text{Au}(100)$ has been studied using synchrotron radiation photoemission. Between 1 and 5 ML, the overlayers exhibit changes in the Ni 6 eV satellite with overlayer thickness that indicate a change from atomic to many-electron behaviour. The Ni satellite photoemission intensity is enhanced by at least a factor of 2.0 relative to the Ni 3d band for films of 1 ML compared with bulk Ni(100). The photon energy at which the satellite exhibits a maximum intensity increases monotonically from 66 eV for a 1 ML Ni film to 69–70 eV for a 5 ML film. These results are discussed in terms of the present theories of the origin of photoemission many-body satellites.

1. Introduction

The 6 eV satellite of Ni and of Ni compounds is among the most widely studied many-electron effect in photoemission [1–20]. As interest in lower-dimensional systems (for a review and extensive references see [21]) and magnetic overlayers [22] has increased in recent years, several reports have been published of investigations of the band structure of thin metal overlayer systems (see, e.g. [23]). The present report concentrates on how the known photoemission many-body effects of Ni depend on the Ni overlayer thickness. The present results are, to the best of the authors' knowledge, the first report that the many-body phenomena associated with photoemission from Ni depends on the thickness of the Ni layer.

The details of the many-body phenomena observed in Ni photoemission have been previously reported by other investigators [1–20]. Essentially, what is observed experimentally for bulk Ni is a resonant enhancement of a many-body satellite in the Ni photoemission spectrum at the photon energy corresponding to the Ni 3p core-level-to-Fermi-edge transition [24]. The precise energy of the Ni many-body satellite has been reported variously between 6.0 and 6.8 eV [17, 18]. The Ni 3d band features exhibit an antiresonant dip at photon energies just below the resonant enhancement of the satellite [1–20, 24]. For Ni-containing insulator compounds, such as NiO and NiCl_2 , the Ni 3d band features exhibit a Fano-type antiresonance–resonance enhancement at a photon energy of between 60 and 70 eV. The same materials also exhibit the many-body satellite at the same photon energy and approximately the same binding energy [1–20, 24].

The present theoretical framework for Ni overlayers of 1–4 monolayers (ML) has been presented by several workers [25]. The pertinent points are that the Ni conduction band is predicted to be effectively uncoupled with that of a noble-metal substrate, that

the Ni conduction band is narrower than that of bulk Ni and that the magnetic moment per atom should be enhanced [26].

We present results for Ni overlayers grown epitaxially on Cu₃Au(100). This surface is a classic order–disorder alloy [27] and has been extensively studied by several investigators [28], including two of the present authors [29]. The Ni overlayers, which are deposited epitaxially (*vide infra*), possess a lattice spacing larger than bulk Ni but retain the FCC crystal structure. The lattice mismatch between Ni(100) and Cu₃Au(100) is 6–7% [30].

The remainder of this paper discusses the methodology (section 2), the results (section 3) and the conclusions obtained (section 4).

2. Methodology

The present report presents data indicating a qualitative change in both the Ni 3d band and the many-body satellite as a function of Ni overlayer thickness. Ni overlayers between 1 and 5 ML thick were deposited on a clean and well ordered Cu₃Au(100) substrate, as confirmed by LEED and the Auger technique. Residual contamination was oxygen at the level of at most 2 at.% on the surface. The Ni overlayers were deposited in a vacuum chamber with a base pressure of 1.0×10^{-10} Torr. The pressure rise during deposition was 1.0×10^{-10} Torr or less. The overlayer films were examined using LEED, the Auger technique and angle-resolved photoemission. The films were well ordered, with several orders of LEED spots 1–1.5 mm in size on a 120° LEED screen, except for the thickest film, which exhibited LEED spots 4 mm in size and greatly increased diffuse scattering, both indicating a film possessing appreciable disorder. Auger spectra demonstrated that the films were clean, with contamination, predominantly oxygen, of less than 1 at.%. The overlayer film thickness was obtained from Auger peak height analysis and thin-film monitoring measurement and the thicknesses quoted are only accurate to within $\frac{1}{2}$ ML.

The Ni 6 eV satellite overlaps, in energy, an Au surface state and part of the Au d band [30–32]. Although the Au state and the Ni satellite do not mix (symmetry forbidden), for 1–2 ML Ni films both are visible. To ensure an accurate estimate of the Ni satellite intensity, we carefully studied the clean Cu₃Au(100) substrate over the same photon energy range as used to study the Ni satellite. Further, we have compared the intensity ratio of the Ni satellite to Ni 3d band in two ways. We compared 1 and 2 ML Ni films, in which the Au features are visible, and, separately, 3–5 ML Ni films, which do not exhibit the Au features. The results are presented below. All spectra shown are the raw data, without smoothing or background subtraction.

3. Results

Figure 1 illustrates a series of spectra obtained for a 1 ML Ni overlayer at normal emission for photon energies between 62 and 74 eV, encompassing the Ni 3p threshold. The photon energy is labelled for each spectrum. The position of the satellite is indicated

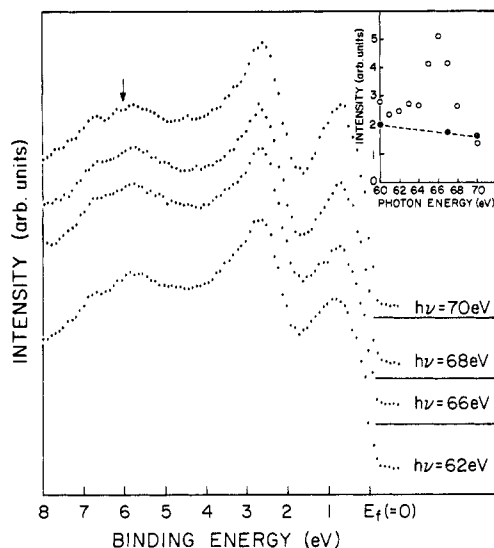


Figure 1. Normal emission photoemission spectra taken for a 1 ML Ni overlayer on $\text{Cu}_3\text{Au}(100)$. The arrow highlights the 6 eV satellite location. The inset illustrates the integrated intensity of the spectral intensity between 5.6 and 7.2 eV for the Ni films (open circles) and clean $\text{Cu}_3\text{Au}(100)$ (full circles).

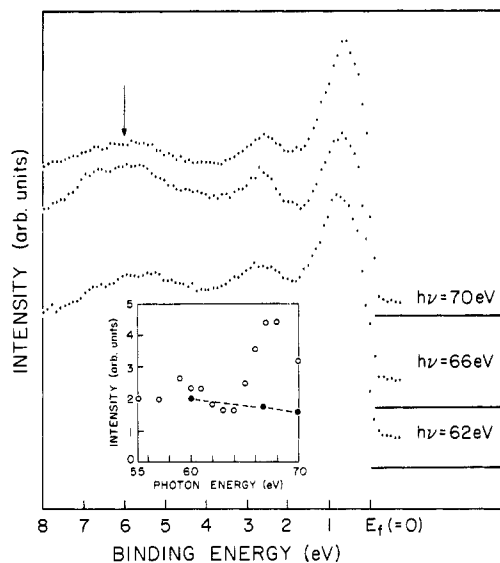


Figure 2. Normal emission photoemission spectra taken for a 3 ML Ni overlayer on $\text{Cu}_3\text{Au}(100)$. The arrow highlights the 6 eV satellite location. The inset illustrates the integrated intensity of the spectral intensity between 5.6 and 7.2 eV for the Ni films (open circles) and clean $\text{Cu}_3\text{Au}(100)$ (full circles).

with an arrow. All spectra are normalised to the height of the Cu 3d band. The inset shows the integrated relative intensity of the spectra between 5.6 and 7.2 eV binding energy as open circles. We followed the same procedure for the clean $\text{Cu}_3\text{Au}(100)$ substrate. The inset shows the results (full circles) for clean $\text{Cu}_3\text{Au}(100)$. This figure and inset demonstrate that, even for a 1 ML Ni film, the Ni 6 eV satellite dominates the 5.6–7.2 eV binding energy region across the Ni 3p threshold. Specifically, there is a marked enhancement in this binding energy region across the Ni 3p threshold, and the clean $\text{Cu}_3\text{Au}(100)$ intensity decreases monotonically across this photon energy range.

To determine how the Ni 6 eV satellite changes with overlayer thickness, 1–5 ML Ni films were deposited on the $\text{Cu}_3\text{Au}(100)$ substrate and spectra obtained for a range of photon energies encompassing the Ni 3p threshold. Figures 2 and 3 illustrate the spectra obtained for a 3 ML Ni overlayer and a 5 ML Ni overlayer, respectively. In each figure, the inset illustrates the integrated relative intensities for 5.6–7.2 eV binding energies (open circles). The clean substrate are included in the inset (full circles) for comparison. What emerges from these results is that all Ni films, including the 1 ML films, exhibit an enhancement of the 6 eV satellite across the Ni 3p threshold. The spectra in figure 3 (5 ML Ni films) illustrate why the 5.6–7.2 eV binding energy region was chosen; this region encompasses the Ni satellite peak. Figure 3 also illustrates the abrupt nature of the satellite resonance and the extended structure at a higher binding energy for photon energies above the resonance threshold.

To determine how the Ni satellite intensity is affected by the overlayer thickness, we analysed the above data so as to answer several questions.

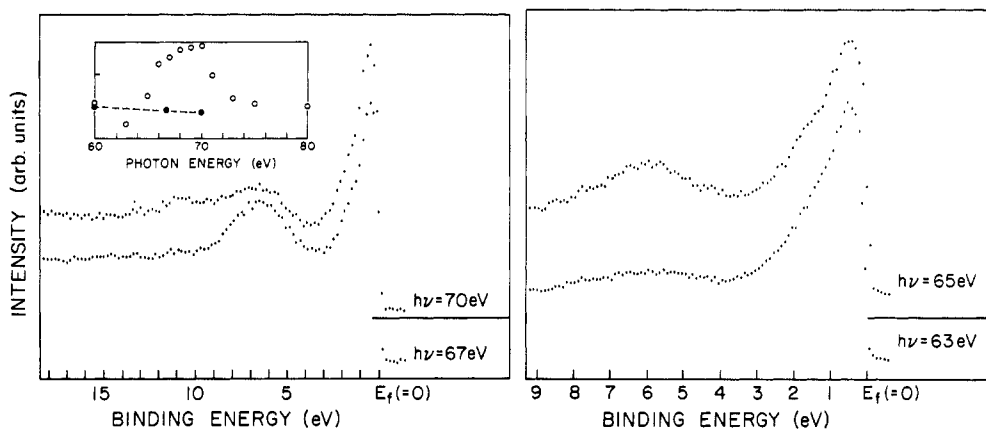


Figure 3. Normal emission photoemission spectra taken for a 5 ML Ni overlayer on $\text{Cu}_2\text{Au}(100)$. The inset illustrates the integrated intensity of the spectral intensity between 5.6 and 7.2 eV for the Ni films (open circles) and clean $\text{Cu}_2\text{Au}(100)$ (full circles). $h\nu = 63$ eV, $h\nu = 65$ eV, a view showing the abrupt onset of the satellite. $h\nu = 67$ eV, $h\nu = 70$ eV, an expanded view showing the structure at higher binding energy.

- (i) How does the integrated intensity ratio of the Ni satellite to Ni 3d band change with overlayer thickness?
- (ii) What is the Ni satellite binding energy and how does it change with overlayer thickness? The 1–2 ML Ni films exhibit a sufficiently high spectral intensity due to the Au to preclude an accurate answer to this question.
- (iii) At what photon energy is the Ni satellite intensity a maximum?
- (iv) How does the Ni 3d band intensity change across the Ni 3p threshold?

Figures 4(A) and 4(B) illustrates the relative integrated intensity ratios of the Ni satellite to Ni 3d band for 1 and 2 ML Ni films and for 3, 4 and 5 ML Ni films, respectively. The uncertainty in the ratio is 1.5 times the sizes off the symbols. As mentioned above, the spectra of the 1–2 ML Ni films exhibit Au spectral density between 5.6 and 7.2 eV binding energy; so we deemed it inappropriate to compare the thinner (1–2 ML) and the thicker (3–5 ML) Ni overlayers with respect to their intensities. The results illustrated in figure 4 indicate that there are changes in the resonant enhancement of the satellite-to-3d ratio between 1 and 2 ML (relative ratios of 1.23 : 1) and 3, 4 and 5 ML (relative ratios of 1.70 : 1.49 : 1).

The Ni satellite binding energy does not depend on the overlayer thickness between 3 and 5 ML, as figures 1–3 illustrate. The photon energy at which the Ni satellite possesses a maximum intensity does change with overlayer thickness, however, as figure 5 illustrates. The Ni satellite exhibits a maximum intensity at 66 eV for a 1 ML Ni overlayer, and the photon energy corresponding to maximum satellite intensity increases monotonically with increasing overlayer thickness to 69–70 eV for a 5 ML Ni overlayer (figure 5(A)).

Figure 5(B) also illustrates the Ni 3d integrated intensity as a function of photon energy for 1 ML and 5 ML Ni overlayers. The results indicate that the 1 ML Ni films exhibit a much less pronounced antiresonant dip than do the thicker films. The photon energy corresponding to the dip in intensity does not appear to change significantly with overlayer thickness.

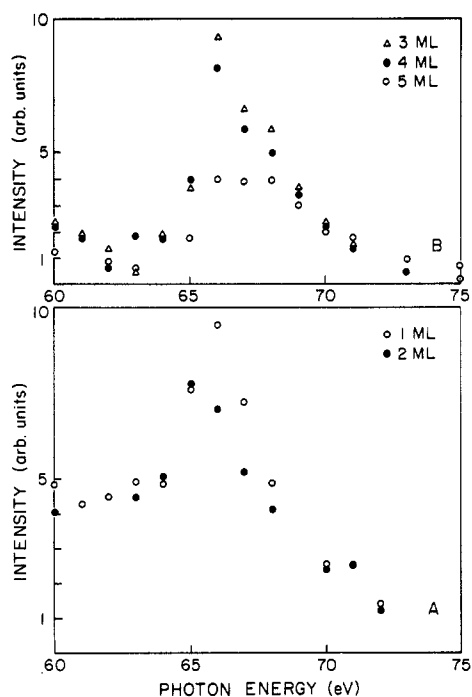


Figure 4. (A) Integrated intensity ratio of the Ni 6 eV satellite to Ni 3d band for 1 ML (open circles) and 2 ML (full circles) Ni overlayers as a function of photon energy. (B) Integrated intensity ratio of the Ni 6 eV satellite to Ni 3d band for 3 ML (open triangles), 4 ML (full circles) and 5 ML (open circles) Ni overlayers as a function of photon energy.

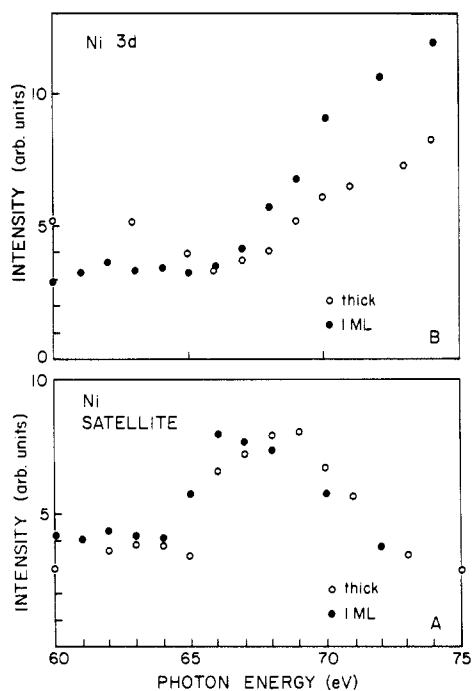


Figure 5. (A) Ni satellite integrated intensity for 1 ML (full circles) and 5 ML (open circles) Ni overlayers as a function of photon energy. (B) Ni 3d band integrated intensity for 1 ML (full circles) and 5 ML (open circles) Ni overlayers as a function of photon energy.

4. Discussion and conclusions

The results indicate that the ratio of the Ni 6 eV satellite to 3d band increases by at least a factor of 2.0 as the Ni overlayer thickness decreases from 5 ML to 1 ML. This is qualitatively in accord with the current theoretical understanding of the origin of the 6 eV satellite [18, 20]. The relative intensity ratio of the satellite to 3d band is viewed [18, 20] as controlled by the ratio U/W , where U is the electron-hole correlation energy and W is the conduction band width. U is largely of atomic origin while W is controlled by the electron overlap in the solid sample. For Ni overlayers on $\text{Cu}_3\text{Au}(100)$, where the Ni film exhibits a larger lattice constant than bulk Ni, the Ni conduction band width is narrower than that of bulk Ni owing to reduced Ni-Ni orbital overlap. As a result, W will decrease for the thin Ni overlayers. By contrast, U is largely atomic in origin. Although the magnitude of U changes between the atomic and condensed phases, owing to screening, the overlayer thickness should not affect U significantly. The results presented in figures 1–4 are qualitatively in agreement with this prediction. Also noteworthy, however, is the larger ratio for 3 and 4 ML films compared with 5 ML films, where the band widths should, from calculations on similar systems, be almost the same [33–

35]. Unfortunately, no theoretical calculations of this system showing conduction band width versus overlayer thickness are currently available for direct comparison.

In addition to the satellite-to-main-peak ratio, another noteworthy point is the manner in which the satellite intensity itself depends on overlayer thickness. Specifically, the photon energy at which the satellite exhibits a maximum intensity increases monotonically from 66 to 69–70 eV as the overlayer thickness increases from 1 to 5 ML. This result is to be compared with an analogous photon energy of 69–71 eV for bulk Ni [1–18]. By contrast to bulk Ni, atomic Ni possesses an excitation (analogous to the satellite) that exhibits a peak in intensity at a photon energy of 65–66 eV [36]. We conclude that the Ni satellite exhibits an evolution in intensity lineshape and peak intensity similar to the evolution of atomic to bulk Ni as the overlayer thickness increases from 1 to 5 ML. It is noteworthy that such behaviour occurs on a metallic substrate. These results enhance the credibility that the Ni overlayer is, electronically, only very weakly coupled to the substrate, as theoretically predicted [25, 33–35].

Finally, the Ni 3d band exhibits an antiresonant dip in intensity for all overlayers (figure 5), as does bulk Ni [1–20] and Ni compounds [1–20]. The strength of the dip in intensity increases as the overlayer thickness increases. This is a somewhat surprising result since the antiresonant behaviour has been largely attributed to an atomic origin [24]. We can only speculate that the extra-atomic effects, which tend to enhance such an antiresonant dip in intensity, have a stronger influence for the thicker overlayers, where the coordination number and conduction band width are both larger.

In summary, we have presented the results of a first study, to our knowledge, of the changes in a many-body satellite with overlayer thickness. The significant results include the following:

- (i) an enhancement of satellite intensity for thinner overlayers, consistent with theoretical predictions;
- (ii) a monotonic increase in photon energy for maximum satellite intensity with increasing overlayer thickness, consistent with an evolution in satellite character from atomic to bulk Ni;
- (iii) an enhancement of the antiresonant dip in the Ni 3d band intensity with increasing overlayer thickness, for which we conjecture that extra-atomic effects are more effective for thicker overlayers.

What has been established is that the classic Ni many-body satellite is influenced by overlayer thickness, and that such studies are a promising line of inquiry for the influence of reduced dimensionality on many-body effects.

Acknowledgments

We benefited from conversations with Peter Dowben. G King Walters kindly lent us the Cu₃Au(100) sample. The US Department of Energy provided financial support. The work was performed at the Wisconsin 1 GeV synchrotron, a facility supported by the National Science Foundation. Ed Rowe and the optics staff members were particularly helpful.

References

- [1] Baer Y, Heden P F, Hedman J, Klasson M, Nordling C and Siegbahn K 1970 *Phys. Scr.* 1 55

- [2] Hufner S and Wertheim G K 1975 *Phys. Lett.* **51A** 299
- [3] Guillot C, Ballu Y, Paigne J, Lecante J, Jain K P, Thiry P, Pinchaux R, Petroff Y and Falicov L M 1977 *Phys. Rev. Lett.* **39** 1632
- [4] Barth J, Kalkoffen G and Kunz C 1979 *Phys. Lett.* **74A** 360
- [5] Penn D R 1979 *Phys. Rev. Lett.* **42** 921
- [6] Liebsch A 1979 *Phys. Rev. Lett.* **43** 1431
- [7] Eberhardt W and Plummer E W 1980 *Phys. Rev. B* **21** 3245
- [8] Barth J, Gerken F, Kobayashi K L I, Weaver J H and Sonntag B 1980 *J. Phys. C: Solid State Phys.* **13** 1369
- [9] Davis L C and Feldkamp L A 1981 *Phys. Rev. B* **23** 6239
- [10] Clauberg R, Gudat W, Kisker E, Kuhlmann E and Rothberg G M 1981 *Phys. Rev. Lett.* **47** 1314
- [11] Oh S-J, Allen J W, Lindau I and Mikkelsen Jr J C 1982 *Phys. Rev. B* **26** 4845
- [12] Parlebas J C, Kotani A and Kanamori J 1982 *Solid State Commun.* **41** 439
- [13] Sugawara H, Kakizaki A, Nagakura I and Ishii T 1982 *J. Phys. F: Met. Phys.* **12** 2929
- [14] Kakizaki A, Sugeno K, Ishii T, Sugawara H, Nagakura I and Shin S 1983 *Phys. Rev. B* **28** 1026
- [15] Fujimori A, Minami F 1984 *Phys. Rev. B* **30** 957
- [16] Kato H, Ishii T, Masuda S, Harada Y, Miyano T, Komeda T, Onchi M and Sakisaka Y 1985 *Phys. Rev. B* **32** 1992
- [17] Sakisaka Y, Komeda T, Onchi M, Kato H, Masuda S and Yagi K 1987 *Phys. Rev. Lett.* **58** 733
- [18] Raaen S and Murgai V 1987 *Phys. Rev. B* **36** 887
- [19] Fujimori A, Terakura K, Taniguchi M, Ogawa S, Suga S, Matoba M and Anzai S 1988 *Phys. Rev. B* **37** 3109
- [20] Nolting W, Borgiel W, Dose V and Fauster Th 1989 *Phys. Rev. B* **40** 5015
- [21] Dowben P A, Onellion M and Kime Y J 1988 *Scanning Microsc.* **2** 177
- [22] Thompson M A and Erskine J L 1985 *Phys. Rev. B* **31** 6832
- [23] Kamper K P, Schmitt W and Guntherodt G 1988 *Phys. Rev. B* **38** 9451
- [24] For a discussion of such enhancements, see [18] for a recent perspective. Also, see the classic work by Fano U 1961 *Phys. Rev.* **124** 1866
- [25] Fu C L, Freeman A J and Oguchi T 1985 *Phys. Rev. Lett.* **54** 2700
- [26] Erskine J L 1980 *Phys. Rev. Lett.* **45** 1446
- [27] Buck T M, Wheatley G H and Marchut L 1983 *Phys. Rev. Lett.* **51** 43, and earlier pertinent references therein
- [28] Sundarem V S, Alben R S and Robertson W D 1974 *Surf. Sci.* **46** 653
- [29] Chen Qibiao and Onellion M unpublished
- [30] Graham G W 1984 *Surf. Sci.* **184** 137
- [31] Jordan R G, Sohal G S, Gyorffy B L, Durham P J, Temmerman W M and Weinberger P 1985 *J. Phys. F: Met. Phys.* **15** L135
- [32] Wang Z Q, Wu S C, Quinn J, Lok C K C, Li Y S, Jona F and Davenport J W 1988 *Phys. Rev. B* **38** 7442
- [33] Wang D, Freeman A J and Krakauer H 1981 *Phys. Rev. B* **24** 1126
- [34] Tersoff J and Falicov L M 1982 *Phys. Rev. B* **26** 6186
- [35] Huang H, Zhu X and Hermanson J 1984 *Phys. Rev. B* **29** 2270
- [36] Schmitt E, Schroder H, Sonntag B, Voss H and Wetzell H E 1983 *J. Phys. B: At. Mol. Phys.* **16** 2961